Chapter 4 – Near Fault Ground Motion

4.1 Introduction

This chapter deals with the description of near-source ground motions and their characteristics which make them different from far-field ground motions.

4.2 Source to Site Effects

Ground motion at a particular site due to earthquakes is influenced by source, travel path and local site conditions. The first relates to the size and source mechanism of the earthquake. The second describes the path effect of the earth as waves travel at some depth from the soil to the site. The third describes the effects of the upper hundreds of meters of rock and soil and the surface topography at the site. Strong ground shakings cause severe damage to man-made facilities and unfortunately, sometimes, induce losses of human lives.

Local site conditions can profoundly influence all the important characteristics- amplitude, frequency, content and duration- of strong ground motion. The extend of their influence depends on the geometry and material properties of the subsurface materials, on site topography and on the characteristics of the input motions. The nature of the local site effects can be illustrated in several ways: by simple, theoretical ground response analyses, by measurements of actual surface and subsurface of the same site, and by measurements of ground surface motions from sites with different subsurface conditions.

The characteristics of seismic waves are altered as they travel from the source to the site of civil engineering works, due to wave dispersion at geological interfaces, damping and changes in the wave front shape. The latter are referred to as ‘distance and travel path effects’ . Moreover, local site conditions may affect significantly the amplitude of earthquake ground motions; these are known as ‘site effects’. Non - linearity of soil response and topographical effects may also influence ground - motion parameters.

It has been demonstrated that the most important topographical parameter influencing local amplification of ground motion is the steepness of the ridge (Finn, 1991). Consequently, as the ridge becomes steeper, the displacement amplification increases.
Measured amplification at hill crests with respect to the base ranges between 2 and 20. The latter values are higher than those predicted analytically (generally between 2 and 4) because of the significant influence of both ridge-to-ridge interaction and three dimensional effects.

4.3 Directional effects

Earthquakes of small magnitude are frequently generated by sources that may be represented by a point, since the fault rupture extends only a few kilometers. Conversely, for large earthquakes, fault rupture traces can be a few hundred kilometers long. In the latter case, seismic wave radiation is influenced by the source dimensions. Earthquake stress waves propagate in the direction of faulting more intensely than in other directions. This affects the distribution of shaking intensity and hence the distribution of
ground - motion parameters and consequently damage distribution. For example, waves propagate away from the fault rupture with different intensity along different directions; this observation is referred to it as “directivity”.

Benioff (1955) and Ben - Menachem (1961) demonstrated that such directivity can lead to azimuthally differences in ground motions. Directivity occurs because fault ruptures are moving wave sources, which travel at a finite velocity along the fault. The engineering implication of such directivity effects is that sites that are equidistant from the source will be subjected to varying degrees of shaking from the same earthquake. In Figure 4.1 , a pictorial representation of directivity effects on ground motions at sites in the direction of, and away from, fault rupture is given. As the fault rupture (or earthquake source) moves away from the epicenter, it generates ground motion from each segment of
the breaking fault. The ground motion radiates outward in all directions and the seismic energy propagates through expanding wave fronts.

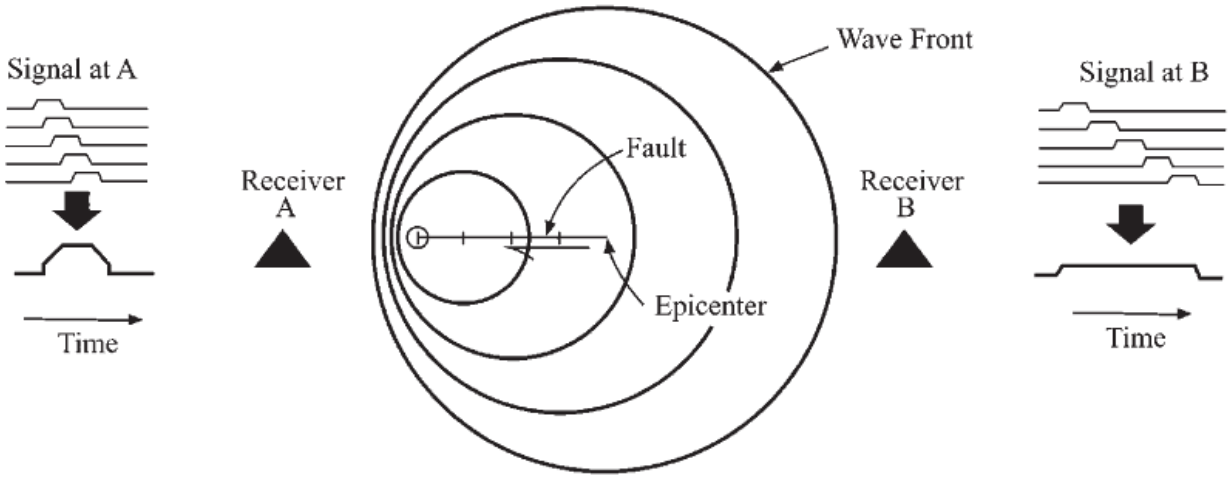

Figure 4. 1 - Directivity effects on sites towards and away from direction of fault rupture (*adapted from* Singh,1985)

From seismic recording three different types of directivity effects have been observed. These effects are depend on the location of the site with respect to the fault and the direction of rupture propagation along the fault, each of them have been explained below.

4.4 Faulting

When two groundmasses move with respect to one another, elastic strain energy due to tectonic processes is stored and then released through the rupture of the interface zone. The distorted blocks snap back towards equilibrium and an earthquake ground motion is produced. This process is referred to as ‘ elastic rebound ’ . The resulting fracture in the Earth ’ s crust is termed a ‘ fault ’ . During the sudden rupture of the brittle crustal rock, seismic waves are generated. These waves travel away from the source of the earthquake along the Earth ’ s outer layers. Their velocity depends on the characteristics of the material through which they travel. The characteristics of earthquake ground motions are affected by the slip mechanism of active faults. Active faults may be classified on the basis of their geometry and the direction of relative slip. The parameters used to describe fault motion and its dimensions are as follows:

- *Azimuth* (φ): the angle between the trace of the fault, i.e. the intersection of the fault plane with the horizontal, and the northerly direction ($0\,^\circ \leq \varphi \leq 360\,^\circ$). The angle is measured so that the fault plane dips to the right - hand side;
- *Dip* (δ): the angle between the fault and the horizontal plane ($0\,^\circ \leq \delta \leq 90\,^\circ$);
- *Slip or rake* (λ): the angle between the direction of relative displacement and the horizontal direction ($-180\,^\circ \leq \lambda \leq 180\,^\circ$). It is measured on the fault plane;
- *Relative displacement* (Δu): the distance travelled by a point on either side of the fault plane. If Δu varies along the fault plane, its mean value is generally used;
- *Area* (S): surface area of the highly stressed region within the fault plane.

The orientation of fault motion is defined by the three angles φ , δ and λ , and its dimensions are given by its area S as displayed in Figure 4.2 ; the fault slip is measured by the relative displacement Δu . Several fault mechanisms exist depending on how the plates move with respect to one another (Housner, 1973). The most common mechanisms of earthquake sources are described below (Figure 3):

- *Dip - slip faults* : One block moves vertically with respect to the other. If the block underlying the fault plane or ‘ footwall ’ moves up the dip and away from the block overhanging the fault plane, or ‘ hanging wall ’ , normal faults are obtained. Tensile forces cause the shearing failure of normal faults. In turn, when the hanging wall moves upward in relation to the footwall, the faults are reversed; compressive forces cause the failure. Thrust faults are reverse faults characterized by a very small dip. Mid - oceanic ridge earthquakes are due chiefl y to normal faults. The 1971 San Fernando earthquake in California was caused by rupture of a reverse fault. Earthquakes along the Circum - Pacifi c seismic belt are caused by thrust faults;
- *Strike - slip faults* : The adjacent blocks move horizontally past one another. Strike - slip can be right - lateral or left - lateral, depending on the sense of the relative motion of the blocks for an observer located on one side of the fault line. The slip takes place along an essentially vertical fault plane and can be caused by either compression or tension stresses. They are typical of transform zones.

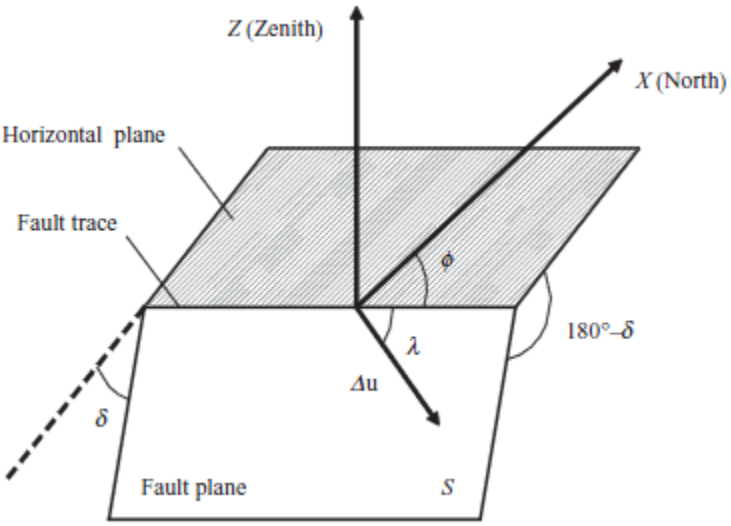

Fig4.2 Parameters used to describe fault motion

Fig4.3

Fundamental fault mechanisms

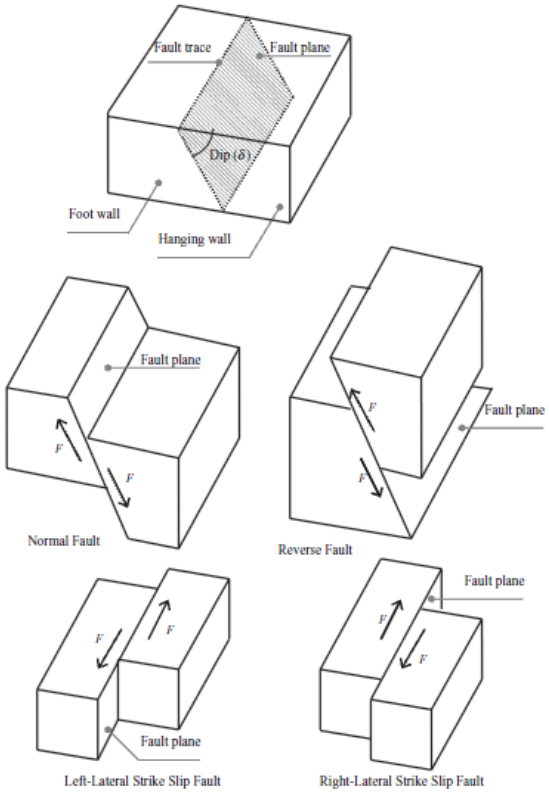

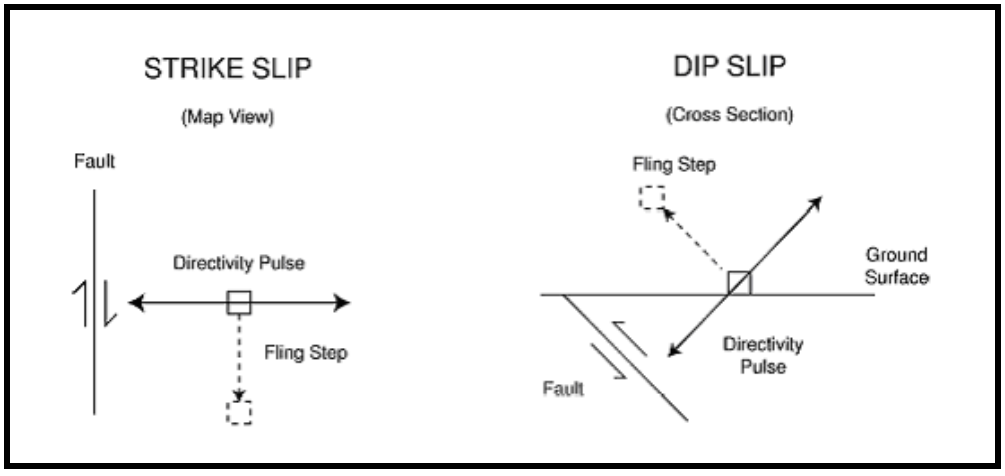

Figure 4.4 Schematic diagram showing the orientations of the fling step and the pulse directivity pattern for horizontal slip (left) and dip-vertical slip (right)

The radiation pattern of shear dislocation on the fault plane tends to orientated the pulse in the direction which is the normal to the fault plane and that is why the fault normal peak velocity is much larger than the fault parallel component. In case of strike slip, the fault normal component and strike normal component are almost equal. Similarly, in dip-slip fault with large dip angle the fault normal component is again represented by the strike normal component. However, in case of small dip-angle the fault normal component is adequately characterized by the vertical component of ground motion.

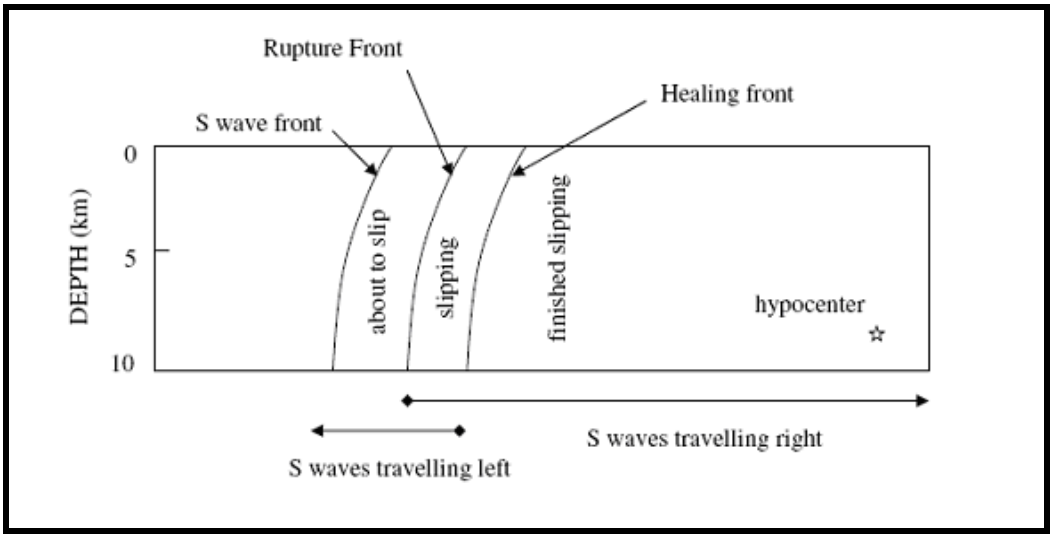

Fig4.5 Schematic diagram of directivity pattern of rupture for a horizontal slip. The illustration shows a snapshot of the forehead rupture at a given time (from Somerville et al 1997a).

For a horizontal mechanism slip (Figure4. 5), when the rupture start and propagates forward (speed approx 80% of the shear wave velocity) away from the fault area and to a region, the energy accumulates near the front intrusion by each successive zone of slip along the fault. The front of the waves reaches a large pulse of motion. The pulse of motion is characterized by the large range intermediate periods and the short duration

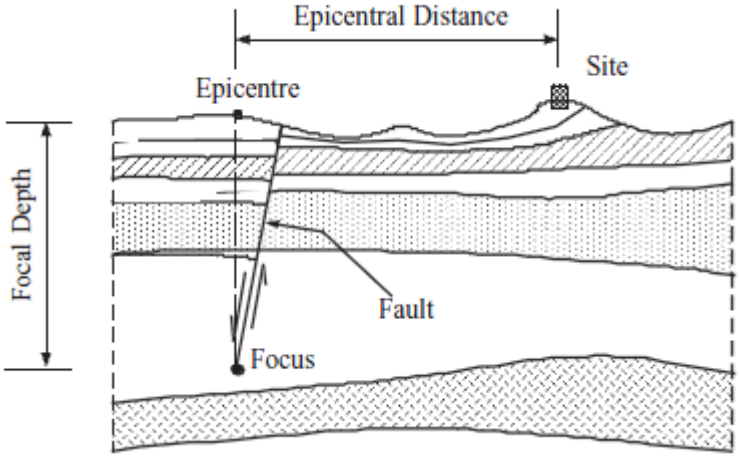

Fig 4.6 Definition of source parameters

The ‘ focus ’ or ‘ hypocentre ’ of an earthquake is the point under the surface where the rupture is said to have originated. The projection of the focus on the surface is termed ‘ epicentre ’ . The reduction of the focus to a point is the point - source approximation (Mallet, 1862). This approximation is used to define the hypocentral parameters. However, the parameters that define the focus are similar to those that describe the fault fracture and motion. Foci are located by geographical coordinates, namely latitude
and longitude, the focal depth and the origin or occurrence time. Figure 4.8 provides a pictorial depiction of the source parameters, namely epicentral distance, hypocentral or focal distance, and focal depth. Earthquakes are generated by sudden fault slips of brittle rocky blocks, starting at the focus depth and observed at a site located at the epicentral distance. Most earthquakes have focal depths in the range of 5 – 15 km, while intermediate events have foci at about 20 – 50 km and deep earthquakes occur at 300 – 700 km underground. The three types are also referred to as shallow, intermediate and deep focus, respectively. Crustal earthquakes normally have depths of about 30 km or less. For example, in Central California the majority of earthquakes have focal depths in the upper 5 – 10 km. Some intermediate - and deep - focus earthquakes are located in Romania, the Aegean Sea and under Spain. The above discussion highlights one of the difficulties encountered in characterizing earthquake parameters, namely the definition of the source. From Figure4.6 , it is clear that the source is not a single point, This has led researchers to propose treatments for point, line and area sources (Kasahara, 1981). It is therefore important to exercise caution in using relationships based on source - site measurements, especially for near - field (with respect to site) and large magnitude events.

The seismic recordings of near field ground motion also exhibits fling step characteristic (discussed in section 4.7) which is a permanent ground dislocation due to the static field distortion of the earthquake. The residual displacement (fling step) appear parallel in the direction of fault rupture, and therefore are not directly related to the above dynamic movement called "pulse directivity effect". In case of horizontal slip (strike-slip) , pulse directivity pattern is displayed on the vertical component and the residual displacement appears in the parallel component. Cracks in vertical dive (dip-slip), both the residual movement and pulse directivity pattern shown in the vertical component. The orientations of the residual movement and pulse directivity pattern for admittance slip horizontal and vertical penetration are shown in Figure4. 7.

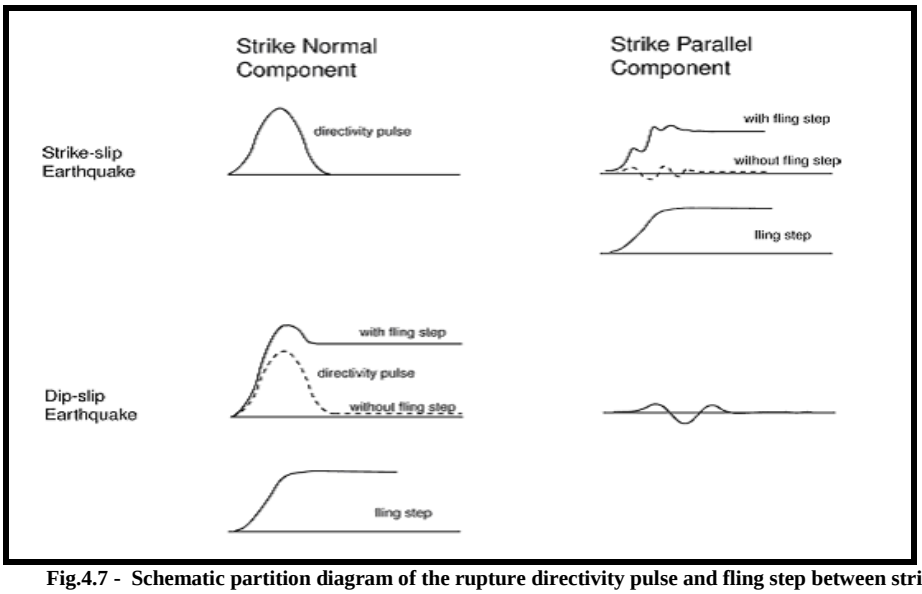

Fig.4.7 - Schematic partition diagram of the rupture directivity pulse and fling step between strike normal and strike parallel components of ground displacement.

Physically, the directivity pattern on ground movements recorded during the earthquake in Loma Prieta, in 1989, as shown in Figure 4.8. The epicenter of the earthquake was near Corralitos and Branciforte Drive, where the horizontal ground displacement are modest and the fault components are vertical as well as horizontal. This is attributed to the backward directivity. At the end of the fault, however, Lexington Dam and the Hollister, the forward directivity causes the horizontal ground movements in normal direction of the fault be pulsed and much larger than the movements of parallel components of the rift. The large pulse movements appear only in perpendicular direction to the rift components (fault normal) of the strike-slip and dip-slip fault.

The effects of directivity pattern of fault rupture may occur both in horizontal slip, and dip-slip strikes. Where fault dip-strike , the conditions frontal directivities shown for areas close to view the top- rift. Mechanisms in horizontal slip, the way shear energy release due to a cross-over rift causes the pulse events oriented perpendicular to horizontal crack (Somerville et al,

1997a).

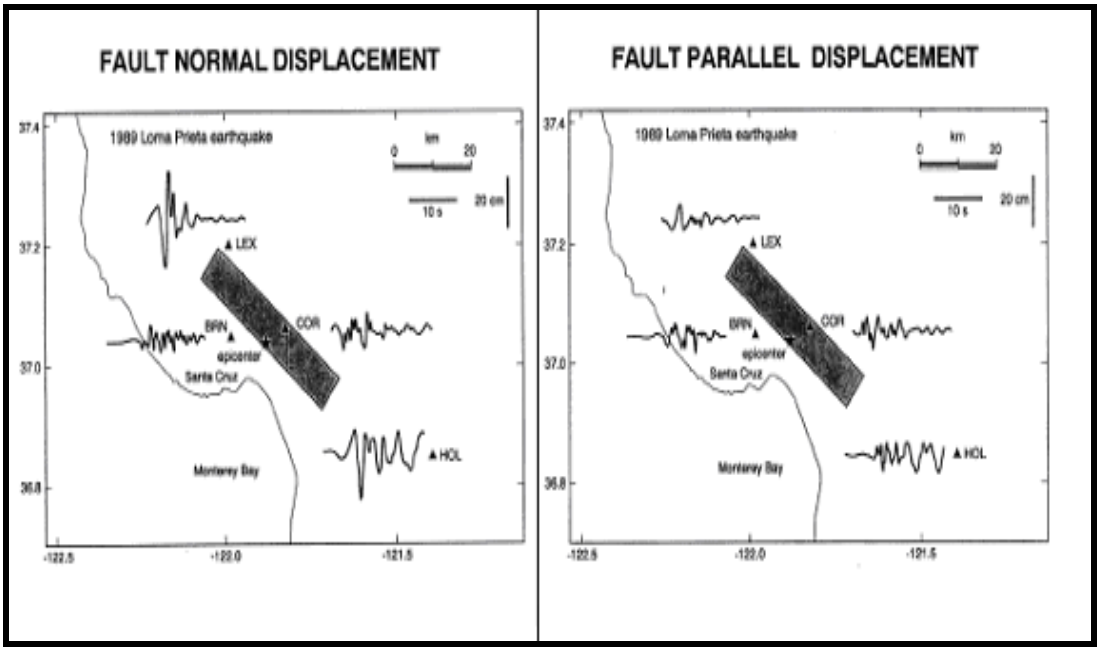

Fig4.8 Loma Prieta 1989 earthquake, Fault rupturing results (directivity effects) for the normal (left) and parallel (right) split components. Source: EERI, 1995

The available data that can be used to measure the effects of the nearby field is limited. However, the recent earthquakes in Turkey and Taiwan have shown a more comprehensive pattern on ground displacement at nearby field. Below are the recorded velocity time history at near source ground motion of different earthquakes.

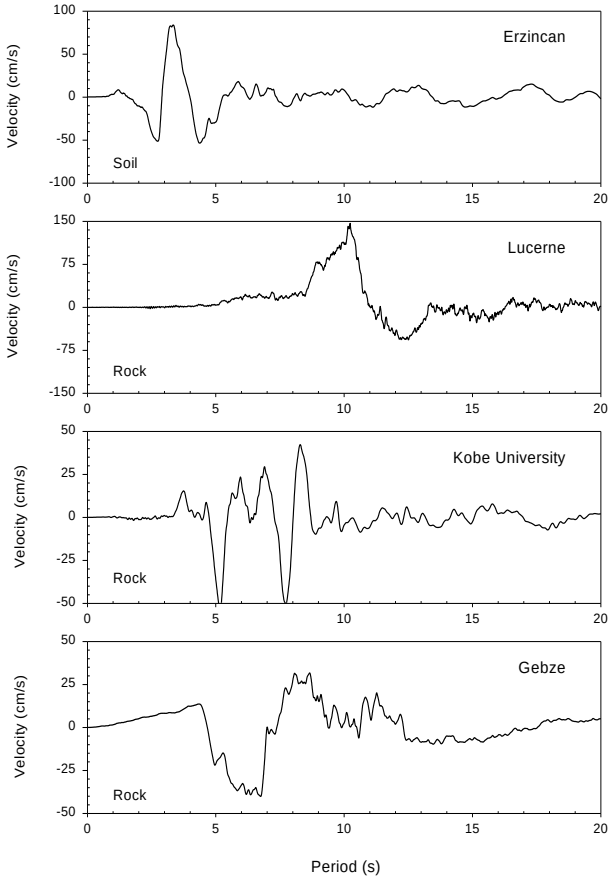

Fig.4.9 - Typical forward-directivity motions recorded in various earthquakes: a) 1992 Erzincan Earthquake, b) 1992 Landers Earthquake, c) 1995 Kobe Earthquake, d) 1999 Kocaeli Earthquake

4.5 Backward Directivity

It has been observed that not all near-fault records have forward directivity effects within an active seismic vicinity. When the rupture propagates away from the site, the ground motion at a site is characterized by long duration and low amplitude at long periods. Such an effect is called as backward directivity.

In Figure 4.8 the ground motion at the BRN and COR exhibits backward directivity and is characterized by long duration motion as opposed to the impulse motion at LUX location where forward directivity is experienced.

4.6 Neutral Directivity

Neutral directivity are observed at sites which are located off to the side of the fault rupture surface when the rupture propagation is neither predominantly towards nor away from the site.

4.7 Fling Step

The fling step involves a large, unidirectional velocity pulse to accommodate this displacement in the slip-parallel direction and is not strongly coupled with the rupture directivity pulse. In strike – slip faulting, the directivity pulse occurs on the strike – normal component component while the fling step occurs on the strike-parallel component. In dip-slip faulting both the fling step and the directivity pulse occur on the strike – normal component. A schematic illustration of the orientation of fling step and rupture directivity pulse are shown in Figure 4.4

The feature of rupture directivity effect, that is most damaging to structures is the large velocity pulse, which can lead to one yield reversal with a large ductility demand. On the other hand, fling step affects the peak velocity and displacement of ground motions. These near fault source effects, which comprise of brief and impulsive ground motions, can not be adequately described in frequency domain which characterizes a uniform distribution of energy throughout the duration of motion. Thus the conventional characterization of design ground motion in the form of response spectra needs to be augmented with a simplified description of the near-source pulses in time domain. A simple characterization is indeed possible with the use of Peak Horizontal Velocity (PHV), approximate period of the dominant pulse (T_V) and the number of significant half-cycles of motion in the larger, fault-normal direction.

4.8 Hanging Wall Effect

The hanging wall effect is primarily due to the proximity of much of the fault to the sites on hanging wall side. It has been observed to have the most pronounced effect for periods shorter than about one second (1s), and at locations away from the top-edge of the fault on the hanging wall side.

The rupture directivity effect, on the other hand, is due to rupture propagation and radiation pattern effect. It is more pronounced for periods longer than 1s, and is concentrated over the top edge of the fault. The relationship between the rupture directivity effect and the hanging wall effect is thus complementary both in the region of influence and the affected period range, thereby increasing the degree of spatial variation of strong ground motion around dipping faults.

Sites on the hanging wall of a dipping fault have closer proximity to the fault as a whole than do the sites at the same closest distance on the foot wall side, tha hanging wall effect is observed to be the greatest in the closest distance range of 8 to 18 km for periods of 0 to 0.6 s and decreases to unity to 5s.

4.9 Ground Motion Parameters

The Somerville *et al* (1997a) parametric conditions leading to forward and backward directivity effects as shown in Figure 4.8, the differentiation in space, the effects of directivity pattern depends on the angle between the direction of rupture propagation and the direction of the waves that travel from the rift in the region (θ for the cracks horizontal slip, and φ for the vertical slip), and from the part of the surface rupture of the fault which is located between the center and the test area (X for the slip horizontal and Y for the vertical fault). To take into account the aforementioned effects of the directivities, Somerville *et al* (1997a) initially expressed the converted medium range values of response spectra (5% damping) with the geometric parameters specified in Figure 10 and the results are shown in Figure 11. The drive ground parameter modified were the horizontal response spectra and the ratio of the fault vertical to horizontal components. These factors are for seismic vicinity of distances less than 15 km and for three different types of seismic sources type depends on soil conditions (Table 4.1). These factors are from UBC (1997) regulation, compatible with the average vertical to horizontal component model Somerville et al (1997a), and therefore, the provisions of the regulation do not examine the greater vertical component of motion Somervilille(1998)

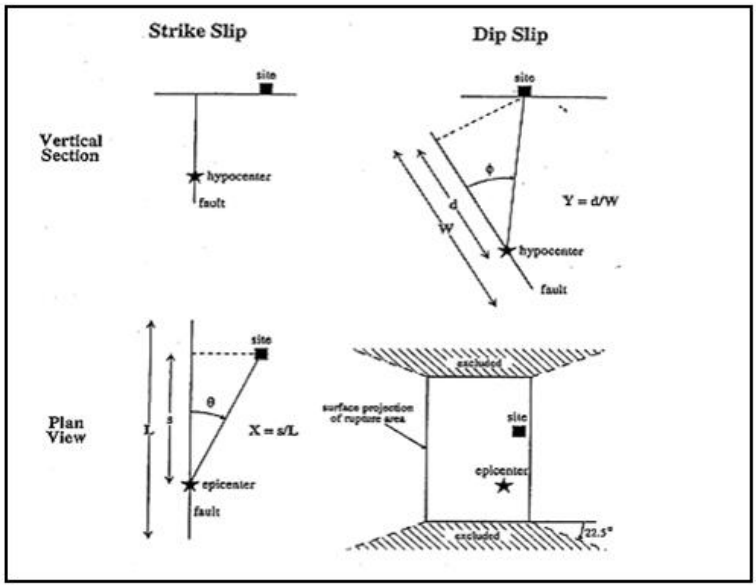

Fig4.10 - : Parameters that are used to interpret the conditions of the directivities of fault by Somerville et al (1997)

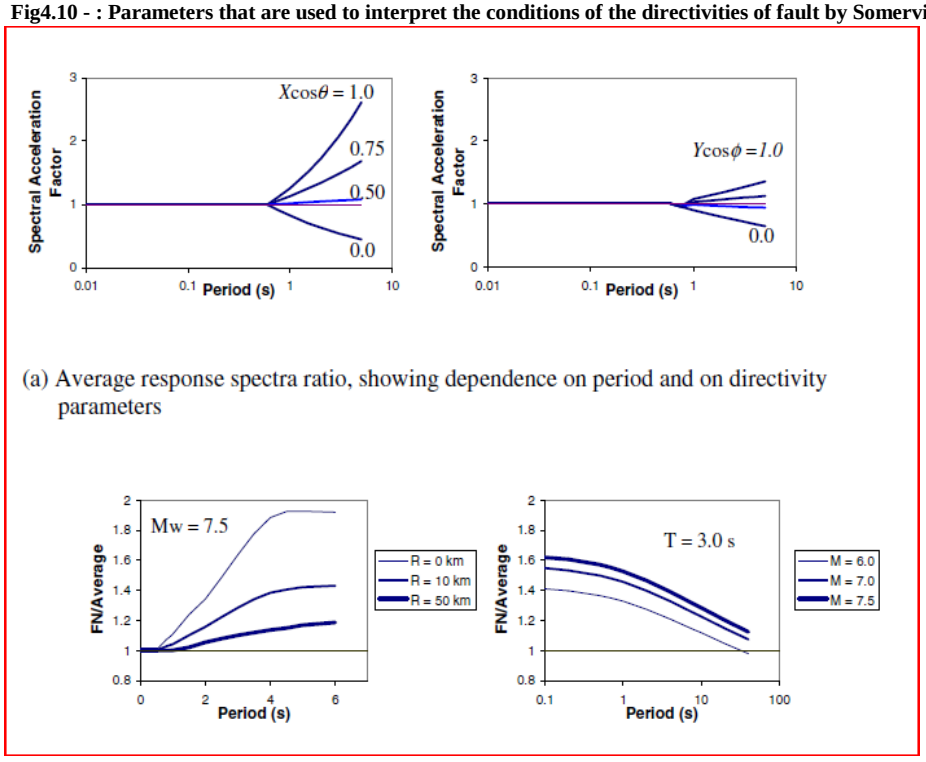

Fig4.11 Estimates of the ratio of Somerville et al (1997 a) between different treaties directivities

a) Near Source Factor (N_a)

Seismic-Source Type	Closest Distance to Known Seismic Source [2,3]		
	≤ 2 km	5 km	10 km
A	1.5	1.2	1.0
B	1.3	1.0	1.0
C	1.0	1.0	1.0

b) Near Source Factor (N_v)

Seismic-Source Type	Closest Distance to Known Seismic Source [2,3]			
	≤ 2 km	5 km	10 km	15 km
A	2.0	1.6	1.2	1.0
B	1.6	1.2	1.0	1.0
C	1.0	1.0	1.0	1.0

c) Near Source Type

Seismic-Source Type	Seismic Source Description	Seismic Source Definition	
		Maximum Moment Magnitude, M	Slip Rate, SR (mm/year)
A	Faults that are capable of producing large magnitude events and which have a high rate of seismic activity	M ≥ 7.0 and	SR ≥ 5
B	All faults other than Types A and C		
C	Faults which are not capable of producing large magnitude earthquakes and which have a relatively low rate of seismic activity	M < 6.5 and	SR ≤ 2

Table 4.1: Near source factor from UBC (1997)

Recent research has established that a time-domain representation of forward directivity ground motion is preferable over frequency-domain representations (Krawinkler and Alavi 1998). This is because traditional response spectrum representations of ground motions do not adequately represent the demand for a high rate of energy absorption represent by near-fault pulses. More specifically, when the high intensity levels of these motions drive structures into the nonlinear range, the linear-elastic assumption underlying the response spectrum concept is invalidated (Somerville 2003). The studies by Krawinkler and Alavi (1998) and Sasani and Bertero (2000) have shown that the simplified version of the pulse velocity can "capture" the obvious characteristics response of structures subjected to ground motion in nearby field. Some Simplified pulses are shown in Figure 4.10. To simulate an impulsive effect to demonstrate, a sine pulse of fault normal component together with the time delay between the start of the vertical and horizontal components of the fault is needed. Table 4.2 provides definitions of common parameters of near fault ground motion, and these parameters are illustrated in Figure 4.11. A simple characterization is possible with the use of maximum horizontal velocity (PHV), the approximate dominate pulse period (T_v), and the number of large in-elastic loop in vertical direction.

The determination of the pulse period uses either the time zero scale (zero crossing time) or the period in which the velocity is equal to 10% of the maximum velocity for this pulse. This is necessary for the pulses to which has been offset by the zero axis in velocity time history. A degree of uncertain in this determination and may lead to variations in the estimates of the T_V . However, the uncertainty associated with the prediction of T_V from seismological variables is much larger than the errors in the calculation of the zero points. The Krawinkler and Alavi (1998) identify the pulse velocity by a clear and comprehensive peak in the response spectrum of the ground motion. Therefore, this estimate of the equivalent pulse period (T_P) is relatively clear. For the ground movement, these different definitions of the period of pulse provide approximately equivalent results. Overall, the ratio between the T_V and $T_{V\text{-}P}$ is 0.84 with a standard deviation 0.28 (Rodriguez- Marek 2000). The coincidence of T_V and $T_{V\text{-}P}$ for a ground motion shows that the pulse velocity contains the energy in a particular zone periods.

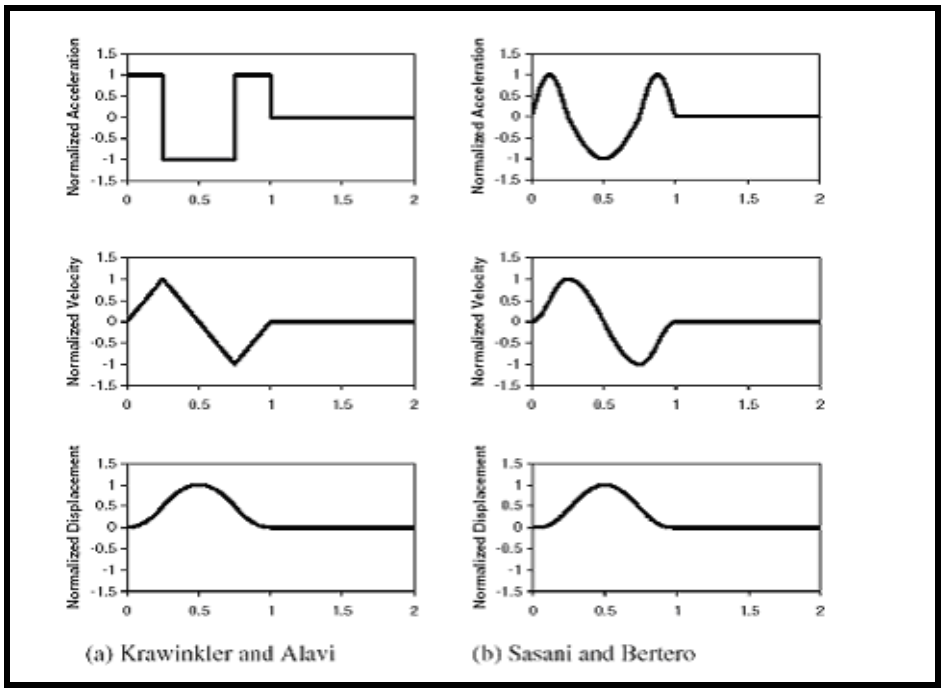

Fig 4.12 Simplified shape of pulses used by researchers

Parameter	Abbreviation	Methodology to obtain parameter
Number of significant pulses.	N	Number of half-cycle pulses in the velocity-time history with amplitudes at least 50% of the peak ground velocity of the record.
Pulse period.	$T_{v,i}$	For each half sine pulse, $T_{v,i} = 2\,(t_2 - t_1)$, where t_1 and t_2 are either the zero-crossing time, or the time at which velocity is equal to 10% of the peak velocity for the pulse if this time is significantly different than the zero crossing time. T_v corresponding to the pulse with maximum amplitude is the overall representative velocity pulse period.
Predominant period from pseudo-velocity response spectra.	$T_{p\text{-}v}$	Period corresponding to a clear and global peak in the pseudo-velocity response spectra at 5% damping.
Pulse amplitude.	A_i	For each half sine pulse, the peak ground velocity in the time interval $[t_1, t_2]$.
Peak ground velocity	PHV	Maximum velocity, defined by the maximum value of A_i. Note, however, that in very few exceptions, the maximum value of A_i in the fault parallel direction does not occur concurrently with the fault normal pulse.
Ratio of fault parallel to fault normal amplitude	$PHV_{P/N}$	Defined by the ratio of maximum A_P divided by maximum A_N, where the subscripts P and N denote fault-parallel and fault-normal motions respectively.
Time delay between fault normal and fault parallel pulse	t_{off}	Time of initiation of fault parallel pulse minus the time of initiation of fault normal pulse.

Table4. 2 Factors used to determine the simplified territorial movements a sine pulse (from Rodriguez-Marek 2000)

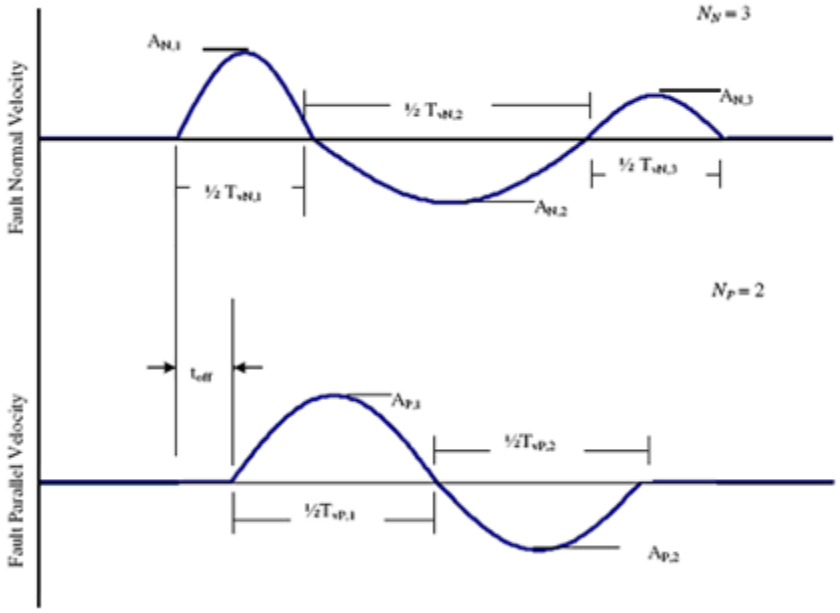

Figure4.13 Factors needed to determine the parallel and perpendicular component of the fault for simplified pulse velocity. The symbols N, P correspond to vertical and parallel movements in the direction of the rift, respectively (Rodriguez-Marek 2000)

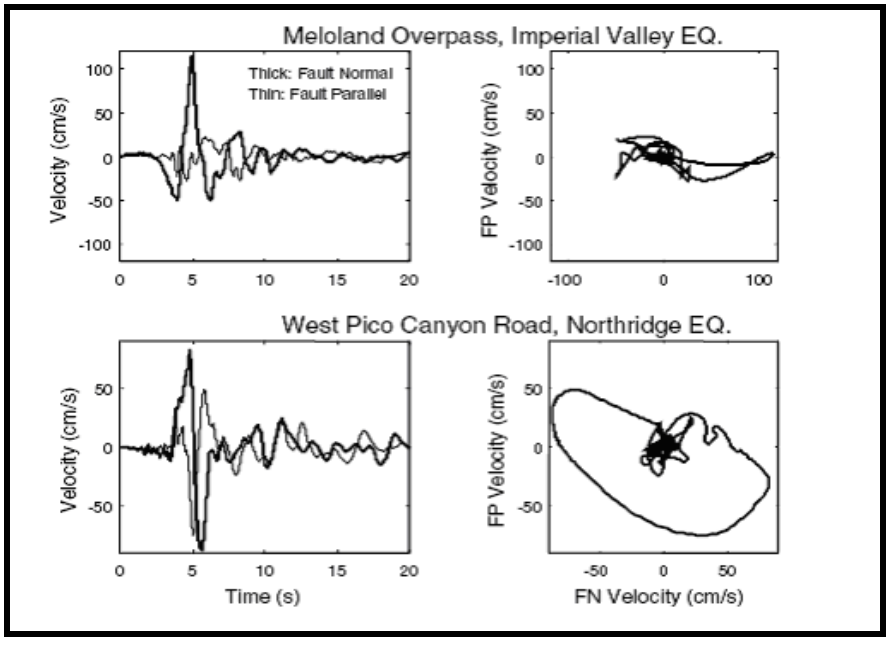

Figure4.14 Velocity time history of fault parallel and normal components of two earthquake in near fault seismic vicinity. It is visible that Meloland, Imperial VAlley EQ has less PF velocity effect as compare to West, Northridge EQ

The study of forward directivity effect on building response in nearby field has been done excessively (e.g. Alavi and Krawinkler 2000). However, there are applications for which the parallel component of fault rupture could also be important. Rodriguez-Marek (2000) employed non-linear analysis to explain that the local soil conditions may have significant effect on values of (PHV) and Tp in both directions of an active fault. Two nearby field recording with significantly different velocity of the fault parallel and normal components are shown in Figure 4.14. Additional research makes it possible to distinguish the results of vibration to addresses the response of soil and building in the near source ground motion. To investigate the impulsive effect of near source ground motion Rodriguez-Marek (2000), presented some simplified intense pulse (Figure 4.15) to used in future earthquake studies.

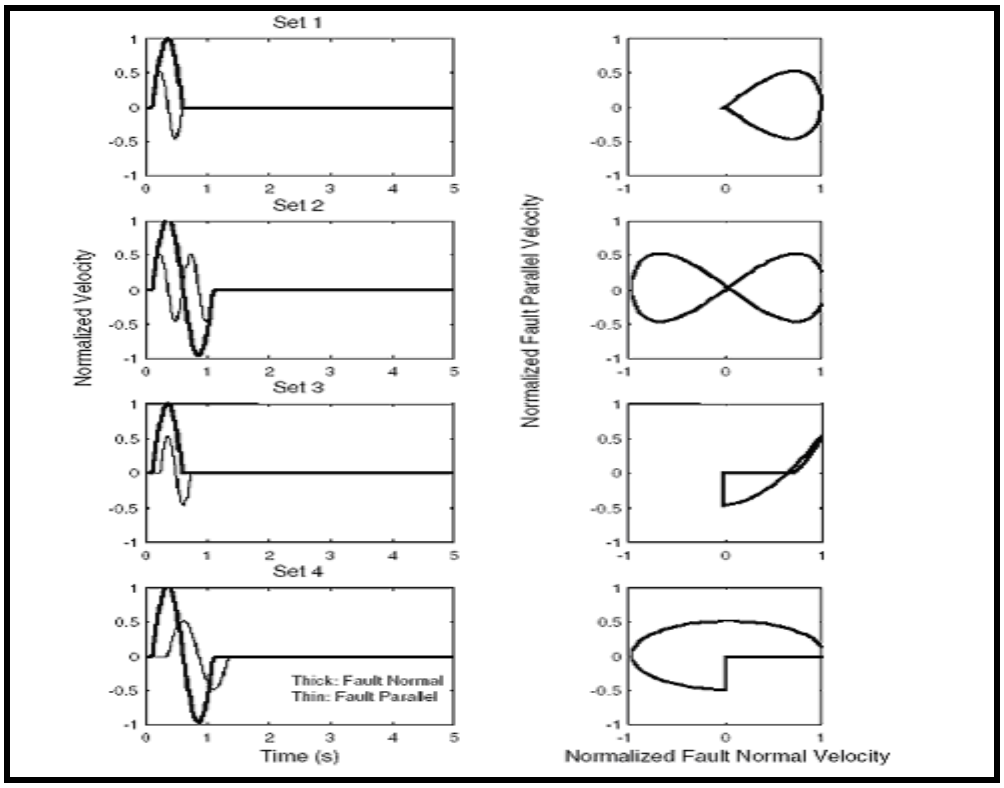

Figure4. 15 Simplified representation of a sine pulse for ground displacement in nearby field. The PHV (maximum horizontal velocity) in fault parallel component accounts for 50% of the fault normal component velocity (Rodriguez-Marek 2000).

4.10 Spectral Acceleration

The Somerville et al (1997a) and Abrahamson (2000) have presented models for the modification of response spectra with damping (ζ=5%) through the damping ratio Abrahamson and Silva (1997). These models were developed with regression variables on geometric parameters of the near field motion as shown in Figure 10. The models are presented for the modification of the geometric mean of the two horizontal components and the ratio of the normal to the average spectral acceleration amplitude. The details of the models shown in the two top rows of Table4.3.

4.11 Duration and an equivalent number of cycles

The Somerville et al (1997a) presented a model for the modification of 5-75% of considerable duration of the damping ratio Abrahamson and Silva (1996). The model was developed with regression variables of geometric parameters of the nearby fault (Figure 10). The model is valid for the duration of the geometric mean of the two horizontal components of the fault. Similar type of model was developed by Liu (2001) for the equivalent number of cycles (N). The details of duration models and number (N) appear in the minimum two rows of Table4. 3

Ground Motion Parameter (Reference)	Description	Equation	Range of Applicability
Spectral Acceleration: Ratio of data/model (Somerville et al., 1997a; Abrahamson, 2000)	y=Bias in average horizontal response spectral acceleration (ln units) with respect to Abrahamson and Silva (1997)	Strike-Slip faults: $y = c_1+1.88c_2 X\cos\theta$ $(X\cos\theta \le 0.4)$ $y = c_1+0.75c_2$ $(X\cos\theta > 0.4)$ Dip-Slip faults: $y = c_1+c_2 Y\cos\phi$	$m > 6.5$ For $m < 6.5$, replace y with $T_m xy$ Where $T_m = 0$ for $m \le 6$ and $T_m = 1+(m-6.5)/0.5$ for $6.5>m>6$ $r < 30$ km For $r > 30$, replace y with $T_d xy$ Where $T_d = 0$ for $r>60$ and $T_d = 1-(r-30)/30$ for $60>r>30$ km
Spectral Acceleration: Ratio of Strike Normal/Average Amplitude (Somerville et al., 1997a)	Natural logarithm of the ratio of strike normal to average horizontal spectral acceleration	$y = \cos 2\xi [C_1 + C_2 \ln(r+1) + C_3(m-6)]$	$6.0 \le m \le 7.5$ $0 \le r \le 50$ km $\xi = \theta$ for strike-slip, ϕ for dip-slip. $0 < \xi < 90°$ C_1, C_2, C_3 function of period. Given separately for cases in which dependence on ξ is included, and cases in which dependence on ξ is ignored.
5-75% sig. duration: Ratio of data/model (Somerville et al., 1997a)	Bias in duration of acceleration with respect to Abrahamson and Silva (1996)	Strike-Slip faults: $y = C_1+C_2 X\cos\theta$ Dip-Slip faults: $y = C_1+C_2 Y\cos\phi$	$6.5 \le m \le 7.5$ $0 \le r \le 20$ km
Number of Cycles (N): Ratio of data/model (Liu et al., 2001)	Bias in N with respect to Liu et al. (2001)	Strike-Slip faults: $y = C_1+C_2 X\cos\theta$ Dip-Slip faults: $y = C_1+C_2 Y\cos\phi$	$6.5 \le m \le 7.5$ $0 \le r \le 20$ km

Table 4.3 Modifying parameters territorial drive for the estimated effects directivity pattern parameters X, Y i f defined in figure 4.7.

The changes in the spectra are shown in Figure 4. 8

4.12 Maximum Horizontal Velocity (PHV)

The maximum horizontal speed (peak horizontal velocity-PHV) strongly influenced by the size, distance, and the ground conditions of the seismic region. The Somerville (1998) proposed to use a two parameter relationship between the logarithm PHV, the size, and the logarithm of the distance.

The Somerrville(1998) performed a regression analysis using a set of 15 near field records as well as 12 artificial near source ground motion. The moment magnitude recordings are in size m=6.2-7.5 and distane r=0-10 km.

To avoid unrealistic forecast of PHV at short distances, the Somerville (1998) used a minimum distance of 3km.

The relationship of Somerville (1998) for the PHV in near to fault vicinity is:

$$\ln(PHV) = -2.31 + 1.15m - 0.50 * \ln(r) \quad \text{(Equation 4.1)}$$

Where r is the minimum distance from the fault but it is limited to at least 3 km.

A similar type of study comparing PHV size and distance was presented by the Alavi and Krawinkler (2000) based on the same data set used by Somerville (1998). The relation of PHV is:

$$\ln(PHV) = -5.11 + 1.59m - 0.58 * \ln(r) \quad \text{(Equation 4.2)}$$

Rodriguez-Marek (2000) ran the regression analyzes using 48 near field velocity time history of 11 earthquake events. The data were for areas with distances r < 20km and m = 6.1-7.4. Separate analyzes were carried out for the recorded displacement on rock and soil. On the basis of the analysis of these recordings, the following relationship for the PHV was proposed:

$$\ln(PHV) = a + b\,m + c \ln(r^2 + d^2) + \eta_i + \varepsilon_{ij} \quad \text{(Equation 4.3)}$$

Where the PHV is in units cm/s, the a, b, c and d are the parameters, r is the minimum distance from the fault , m is size, ηi as an integral and εij is error conditions. The values of parameters of model Rodriguez; Marek (2000) are presented in Table 4.4

Data Set	*a*	*b*	*c*	*d*
All Motions	2.44	0.50	-0.41	3.93
Rock	1.46	0.61	-0.38	3.93
Soil	3.86	0.30	-0.42	3.93

Table 4.4 Parameters of model Rodriguez - Marek (2000) for the PHV.

Figure4. 16 compares the relationship recently proposed by Rodriguez-Marek (2000) with the relations developed by Somerville (1998) and the Alavi and Krawinkler (2000). The relationships differ mainly on the influence of moment magnitude due to the probability the largest amount of the recent study.

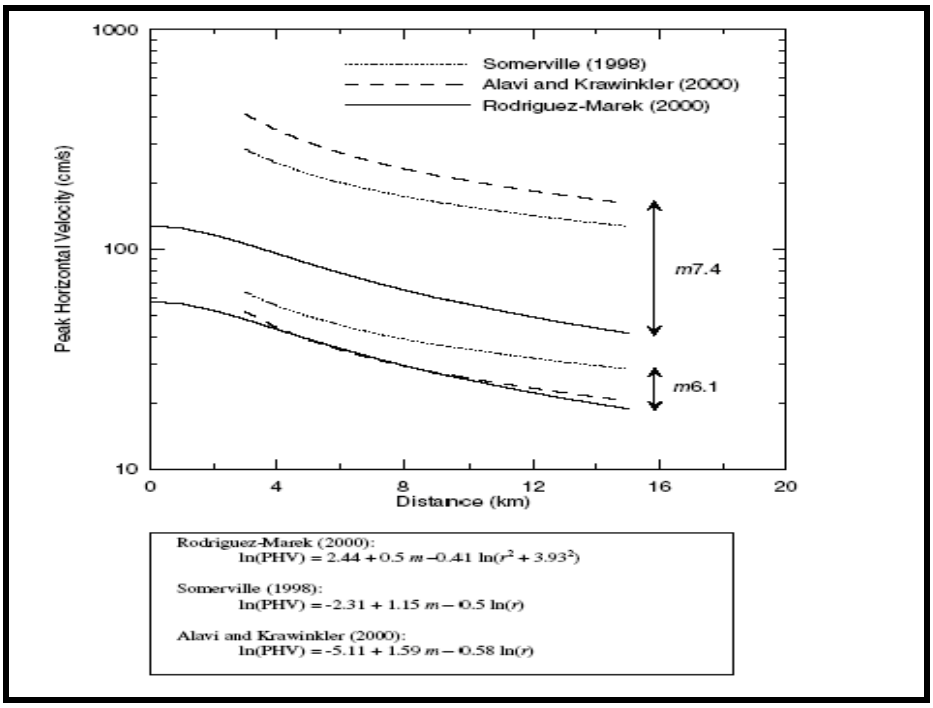

Figure4.16 compares the relationship recently proposed by Rodriguez-Marek (2000) with the relations developed by Somerville (1998) and the Alavi and Krawinkler (2000). The relationships differ mainly on the influence of size m. The differences are probably the largest amount of the recent study.

4.13 Pulse period

The relationship proposed by the Somerville (1998) for the pulse period is:

$$\log_{10}T_p = - 2.5 + 0.425m \quad \textbf{(}\text{Equation 4.4)}$$

Where the T_p is the period of the period of pulse motion and m is the size of the earthquake.

In a larger study of slip distribution using the slip models for 15 earthquakes, the Somerville et al (1999) provide the equation:

$$\log_{10}T_p = -3.0 + 0.5m \quad \textbf{(}\text{Equation 4.5)}$$

The pulse period is linked to the duration of the fault slip, which measures the duration of slip at a specific point on the fault. The relationship between the period of the pulse and the time T_R is (Somerville 1998):

$$T_p = 2.2 * T_R \quad \textbf{(}\text{Equation 4.6)}$$

The relationship between the period of the pulse and the time T_R can also arise from the natural phenomenon of cracking mechanisms. If a crack is modeled as point (point source) and the effects of directivity pattern are missing, the duration of the drive will be equal to the amount of time T_R (Somerville 1998). The used of the fault dimension and the effects of directivity pattern contribute to broadening of the pulse. The duration of the slip to T_r is then, in essence, a lower limit of the period of the pulse.

The Alavi and Krawinkler (2000) determined the pulse period as dominant period range in response speed (T_{V-P}). The relationship which uses this definition for the pulse period is:

$$\log_{10}T_{v-p} = -1.76 + 0.31m \quad \text{(Equation 4.7)}$$

Rodriguez; Marek (2000) developed the following relationship for the pulse period

$$\ln(T_v)_{ij} = a + bm + \eta_i + \varepsilon_{ij} \quad \text{(Equation 4.8)}$$

Where $(T_V)ij$ is the pulse period recording j from the fact I, a and b are the parameters of the model, η_i as an integral and εij is error conditions.

Estimates are provided for the pulse period, T_V, and the dominant period around the pulse range, T_V-p. The values of parameters of the model are presented in Table 4.5. The relationship is valid for m = 6.1 - 7.4 and for r < 20km.

(a) T_v

Data Set	*a*	*b*
All Motions	-8.33	1.33
Rock	-11.10	1.70
Soil	-5.81	0.97

(b) T_{v-p}

Data Set	*a*	*b*
All Motions	-6.92	1.08
Rock	-9.53	1.42
Soil	-5.66	0.91

Table4 .5 Parameters of model Rodriguez - Marek (2000) for the period of the pulse

Figure 4.16 compares the relationship recently proposed by Rodriguez-Marek (2000) with the relations developed by Somerville (1998) and the Alavi and Krawinkler (2000). The relations of the Rodriguez - Marek (2000) for the T_v and T_{v-p} give shorter periods pulse from the relations developed by Somerville (1998) for the T_V and the Alavi and Krawinkler (2000) for T_V-p. The differences are not so great for large sizes earthquake m > 7, where there are uncertainties in the assessment of the period of the pulse.

The influence of soil conditions may be investigated through the use of the relations between Rodriguez - Marek (2000) for a period of the pulse for the rock and the ground (Figure 4. 17). The difference between the prices of the period of the pulse for rock and soil is low for large events (m > 7), but the period of the pulse is greater on soils from that for areas rock for the events with lower sizes. The examination of the classified In pairs stations rock and soil and the effects of non-linear response analysis confirms this observation (Rodriguez - Marek 2000).

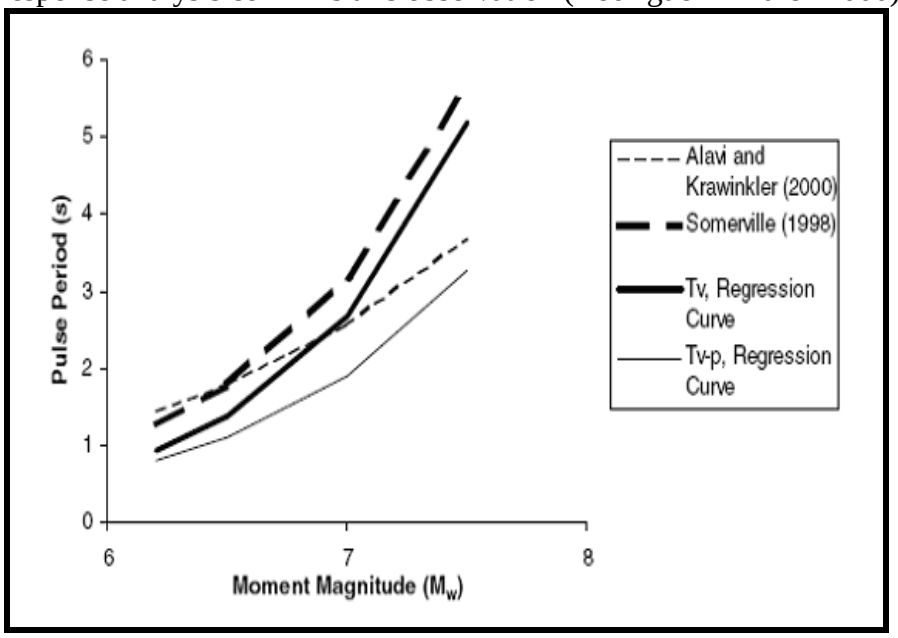

Figure 4.17 Comparison model Rodriguez - Marek with relations developed by Somerville (1998) for the T_V and by Alavi and Krawinkler (2000) for the T_V-p. (Rodriguez- Marek 2000).

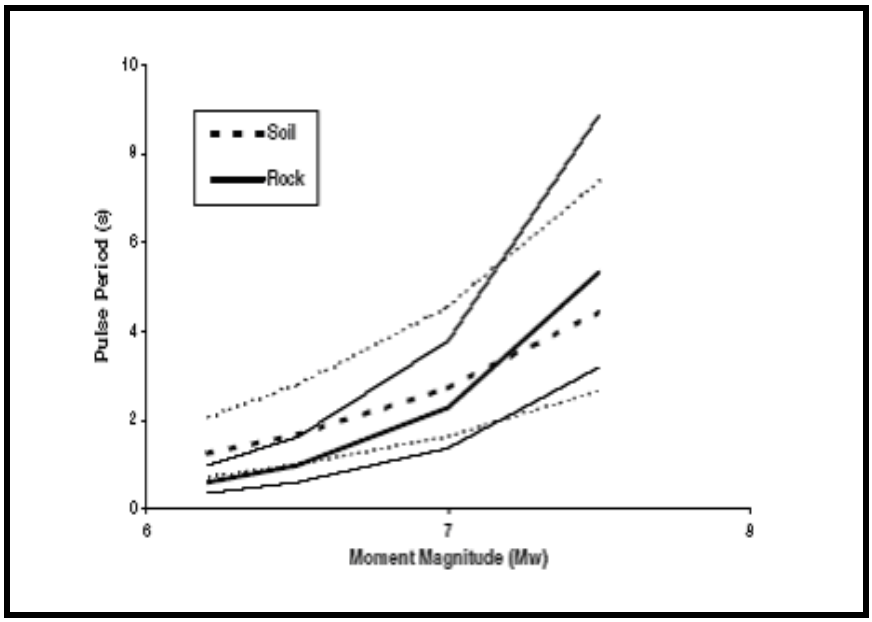

Figure 4.18 Model Rodriguez - Marek for an estimate of the period of the pulse for rock and soil. The sharp curves represent the average value and the thin standard deviations (Rodriguez - Marek 2000)

4.14 Number of pulses

The number of pulses N_v is defined as the number of pulse velocity ranges have at least 50% of the maximum velocity of the ground displace (Table 4.3). For the purposes of calculating the number of major pulse speed, only the fault normal component is consider. The number of pulses in vertical component 48 recordings is shown in table 4.6. Most recordings contain two major pulses (e.g. , a full cycle of ground drive).

The Somerville (1998) suggests that the number of pulses in sine velocity time history to be connected with the number cracks (asperities) in a rift, which then connects with the slip distribution of the fault. There is no model available today for the prediction of the number of large pulses in velocity times histroy. For the most part the Nv will vary between 1 and 3, with Nv = 2 to be a good value used for earthquakes.

Earthquake	Year	Number of Records	Number of Records with given number of half-cycle pulses (N_v)			
			1 pulse	2 pulses	3 pulses	> 3 pulses
Parkfield	66	2	0 (0)	1 (1)	0 (0)	1 (1)
San Fernando	71	1	1 (0)	0 (0)	0 (1)	0 (0)
Imperial Valley	79	13	1 (0)	10 (1)	1 (7)	1 (5)
Morgan Hill	84	2	0 (0)	0 (0)	1 (0)	1 (2)
Superstition Hills(B)	87	2	1 (0)	1 (1)	0 (0)	0 (1)
Loma Prieta	89	8	0 (0)	4 (0)	1 (1)	3 (7)
Erzincan, Turkey	92	1	0 (0)	0 (0)	1 (1)	0 (0)
Landers	92	1	1 (0)	0 (1)	0 (0)	0 (0)
Northridge	94	10	3 (0)	4 (4)	3 (2)	0 (4)
Kobe	95	4	0 (0)	1 (0)	0 (1)	3 (3)
Kocaeli,Turkey	99	4	0 (0)	3 (2)	0 (0)	1 (2)
Totals		48	7 (0)	24 (10)	7 (13)	10 (25)

Table 4.6 Number of pulses (NV) by fact for 48 nearby gound motions (perpendicular to the fault component). The values in parentheses are the numbers of half-cycles of the pulse speed ranges have at least 33% of PHV. (Rodriguez - Marek 2000)

4.15 Effects of the residual Displacement (fling step)

The effects of the residual movement (fling step) as a result of ground mtoion in response of structures were considered less important than the effects of directivity pattern. The recent earthquakes in Turkey (1999) and Taiwan (1999), stressed the importance of the residual deflection associated with the fracture surface on the response of buildings. The distinct tectonic deformation, the differential settlement and the deformation of the ground, there are some aspects of this phenomenon.

The residual movement, resulting static displacement of soil, generally characterized by a pulse speed unidirectional and a fling step in velocity time history. The step in in time history sifts appears to address the rift slip (i.e. , along the intrusion).

For all types fractures, the maximum displacement (MD) of the fault in meters can be linked to the earthquake size (m) via the equation:

$$\log_{10}(MD) = -5.46 + 0.82m \quad \text{(Equation 4.9)}$$

Valid range for earthquake size m= 5.2-8.1, and for MD range from 0.01 m to 14.6 m.

The average displacement (AD) of the fault for all types of fracture is

$$\text{Log}_{10}(AD) = -4.80 + 0.69m \quad \text{(Equation 4.10)}$$

Valid range for earthquake size m = 5.6-8.1

The residual movement of the ground as a result of the rupturing can vary significantly with the distance from the trace of the fault. The tectonic shift away from the rift can be found in traces secondary fractures and other discontinuities.